Available online at www.sciencedirect.com
SCIENCE DIRECT
Polymer 47 (2006) 4282–4291
polymer
www.elsevier.com/locate/polymer

Poly(ε-caprolactone)-*block*-polystyrene metallopolymers via sequential ROP and ATRP condition with in situ generated ruthenium catalyst

Abdiaziz A. Farah, Nicole Hall, Sylvie Morin, William J. Pietro *

Department of Chemistry, York University, 4700 Keele Street, Toronto, Ont., Canada, M3J 1P3

Received 5 December 2005; received in revised form 20 February 2006; accepted 8 March 2006

Abstract

Poly(ε-caprolactone)-*b*-polystyrene with vacant bipyridine coordinating sites and metallated AB type diblock with well-defined metal loci in the polymer chain were synthesized and characterized. Solution atom transfer radical polymerization (ATRP) of styrene where a poly(ε-caprolactone) macromonomer acted as initiator and derivative complex of $[Ru(p\text{-cymene})Cl_2]_2$ as catalyst is reported. ATRP reaction conditions with respect to polymer molecular weights and polydispersity indices (PDI) of the target bifunctional polymers were examined. Electronic absorption and emission spectra of the resultant functional polymers provided evidence of the ruthenium metal chromophores in the diblock copolymer. The thermal properties of all polymers were investigated by differential scanning calorimetry (DSC) and thermogravimetric analysis (TGA), and indicated that they possess a high thermal stability and are miscible in the molten state. The semicrystalline nature of the PCL macroligand and the morphology of thin films of the metal free diblocks were also elucidated by combination of atomic force microscopy (AFM), scanning electron microscopy (SEM) and wide angle X-ray diffraction (WAXD) studies.

Keywords: Poly(ε-caprolactone); ROP; ATRP

1. Introduction

Block copolymers have received much research attention because of their distinct homopolymeric sequences bound covalently at one point. Their importance stems from their unique chemical structures bringing new physical and thermodynamic properties that can be related to their solid-state and solution morphologies [1]. Very often, they exhibit phase separation producing a dispersed phase consisting of one block type in a continuous domain of a second block [2]. Their unusual colloidal, thermal and mechanical properties allow modification of solution viscosity, surface activity, elasticity and impact resistance. Thus, several block copolymers have provided a wide range of materials with tailorable properties depending on the nature and the length of each homopolymer sequence. They found significant practical applications in adhesives [3], sealants [4], surface modifiers for fillers [5], crosslinking agents for elastomers [6], additives for resin gelification and hardening [7], and also as compatibilizing agents for emulsion polymerization [8].

A number of synthetic methodologies have been successfully utilized for the synthesis of block copolymers. These include anionic [9], cationic [10] and coordination polymerization [11]. The emergence of 'living' or controlled radical polymerization affords an important method competitive with others in synthesizing polymers of controlled architectures. In particular, transition-metal-mediated living atom transfer radical polymerization (ATRP) has been used to achieve novel functional polymeric materials with new properties that are directly associated with the precise control of polymer architecture and the predetermined polymer molecular weight and molecular weight distribution (PDI). ATRP is tolerant to many impurities and functional groups, thus allowing its use in synthesizing many functional macromolecules with tailored properties for a range of applications [12]. Furthermore, the design and the study of functional polymers containing metal centers in their structure remains an area of growing interest [13]. Incorporation of transition metals into a polymer microstructure, therefore, offers unique potential for the preparation of processible materials with properties that differ significantly from those of conventional organic polymers. In addition, the diverse range of coordination numbers and geometries which exist for transition elements offer the

* Corresponding author. Tel.: +1 416 736 2100x77700; fax: +1 416 736 5936.
E-mail address: pietro@yorku.ca (W.J. Pietro).

0032-3861/$ - see front matter © 2006 Published by Elsevier Ltd.
doi:10.1016/j.polymer.2006.03.037

possibility of accessing polymers with unusual conformation, mechanical and morphological characteristics [14]. These hybrid organic/inorganic polymers also exhibit attractive electrical, electrochemical, magnetic and optical properties associated with the metal [15]. In particular, the design and the study of functionalized polypyridyl ruthenium (II) metallopolymers is fascinating, as evidence exists that these polymeric materials are expected to have novel electron or energy transfer characteristics [16].

Inspired by the pioneering work of Noels [17] and of Fraser [18], we have prepared the macroligand (**1**) from ring opening polymerization (ROP) of (ε-caprolactone) with a hydroxy functionalized bipyridine initiator catalyzed by $Sn(Oct)_2$ [19]. Macroligand (**1**) with two distinct end functional groups per polymeric chain was converted to tertiary α-bromoester macroinitiator (**2**) for the optimum performance of ATRP [20]. Functional macrointiator (**2**) was then used in solution atom transfer radical polymerization (ATRP) of styrene with in situ generated ruthenium catalyst [$RuCl_2$(*p*-cymene)(PR_3)] to generate AB type poly(ε-caprolactone)-*b*-polystyrene (**4**) with vacant bipyridine binding sites at one polymer chain termini (Scheme 1). The coordination of these novel metal free blocks to solvated $[Ru(bpy)_2(MeOH)_2]^{2+}$ ruthenium species has then generated a linear metallo-diblock (**5**) with well-defined metal domains in the polymer chain. We anticipate that these linear hybrid diblock could provide a wide range of self-assembled structures in solution and in solid-state and the formation of irregular nanoscale substructures by virtue of interaction between the amorphous styrene segments and the semi-crystalline poly(ε-caprolactone) domains in the diblock. Moreover, the precise placement of the metal ion precursors into well-defined block domains will also make these materials unique molecular architectures, providing another key tool for fine-tuning their molecular structure and function.

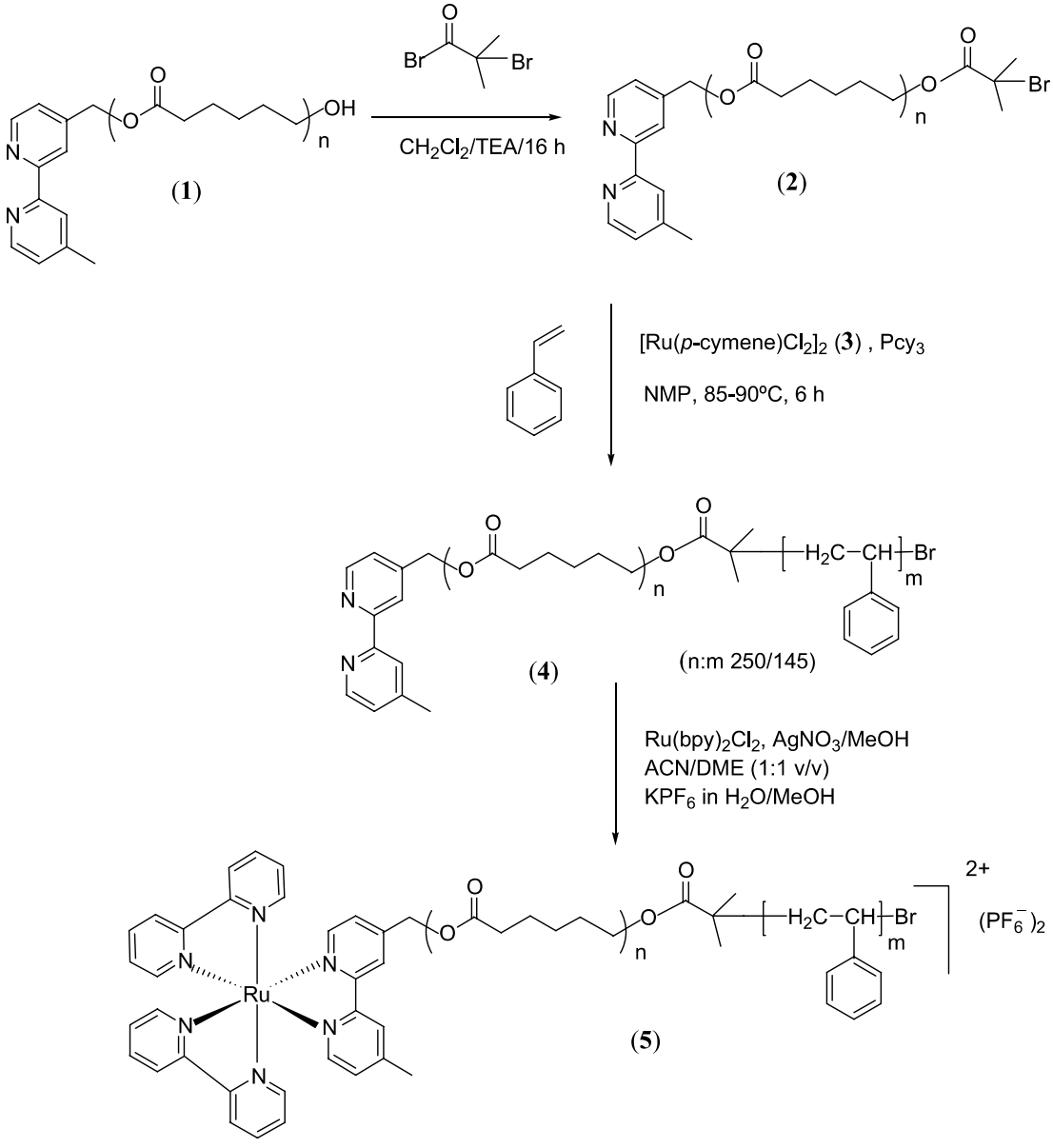

Scheme 1. Synthesis of copolymers (**4**) and (**5**).

In this contribution, we describe the use of poly(ε-caprolactone) macroligand initiator for the ATRP of styrene with in situ generated derivative complex of $[Ru(p\text{-cymene})Cl_2]_2$ for the generation of metal free AB type and linear metallopolymer diblocks. The details of the ATRP reaction conditions, thermal, electronic, emission properties of Ru centered metallopolymer and the morphological properties of metal free diblocks will be described.

2. Experimental

2.1. Methods and materials

All chemicals and solvents were obtained from Aldrich Chemicals Canada and were purified where necessary according to the conventional laboratory techniques [21]. Macroligand (**1**), *cis*-$Ru(bpy)_2Cl_2$ and $[Ru(p\text{-cymene})Cl_2]_2$ (**3**) were prepared as described in [19,22,23], respectively. For column chromatography, high-purity grade (70–230 mesh, 60 Å) silica gel and neutral standard grade (150 mesh, 58 Å) aluminum oxide were used. Infrared spectra were recorded as KBr pellets with Mattson 3000 Fourier transform infrared spectrophotometer. ^1H and ^{13}C NMR spectra were obtained on a Bruker ARX 400 MHz nuclear magnetic resonance spectrometer in an appropriate solvent using tetramethylsilane as an internal standard. Electronic spectroscopy was performed using a Hewlett–Packard 8452 diode array spectrophotometer. Fluorimetry experiments were conducted in a Shimadzu RF 551 fluorimeter on argon or N_2 deareated samples prior to recording. Molecular weights were determined by GPC with a Waters Associates 2690 separation module accessoried inline solvent degasser, a high performance liquid chromatography (HPLC) pump, and an autosampler. The separation module was equipped with a Waters 410 differential refractometer as the concentration detector and, connected in parallel, a Viscotek T60A dual detector consisting of a right-angle laser light scattering detector with a laser source of 670 nm and a four-capillary differential viscometer. Software from Viscotek was used to analyze the data. Columns from Polymer Laboratories with pore sizes of 5×10^2, 1×10^4, and 1×10^5 Å were used with THF as the eluent at a flow rate of 1.0 mL/min. Polystyrene standards purchased from Aldrich and Viscotek were used for calibration. Absolute molecular weights were determined by low-angle laser light scattering (LALLS) performed on a Chromatix KMX-6 instrument at a wavelength of 632.8 nm and a scattering angle of 6–7°. Measurements were carried out at room temperature with a metal cell 4.93 mm long. Each solution was filtered three times through a MILEX filter with an average pore size of 0.2 μm before injection into the cell. The refractive index increment (dn/dc) of the polymer solution was obtained with a Chromatix KMX-16 differential refractometer operating at a wavelength of 632.8 nm. The instrument was calibrated with NaCl solutions. TA instrument DSC 2920 was used to study polymer thermal behavior. The instrument was calibrated with melting transitions of decane and indium, and samples were heated under N_2 atmosphere at a heating rate of 10 °C/min. Reported thermal parameters were taken from the second heating cycle if not otherwise indicated. The glass transition (T_g) value was the mid-point of the heat capacity change whereas the melting point (T_m) was the peak maximum. Thermogravimetric analyses (TGA) were obtained on Perkin–Elmer TGA7 and the temperature was calibrated with the transitions of Perkalloy and Nicoseal. Thermograms were obtained at a heating rate of 20 °C/min under N_2 atmosphere. The X-ray diffraction data were collected using a Bruker AXS Inc. instrument at a radiation wavelength of 1.518 Å, a scan range of 2θ from 1 to 40°, and scan speed of 0.90°/min. The topographic measurements were performed at ambient conditions in air using a commercial AFM (Dimension 3100, NanoScope IIIa, Veeco Instruments) in tapping-mode. Silicon tips with a spring constant of ca. 20–100 Nm^{-1}, a tip radius of ca. 10 nm, and a resonance frequency of about 300 kHz were used for imaging. AFM images were recorded over scan areas of several micrometer squares each with 512×512 data points (or pixels). The AFM images are displayed in the usual way using a grey scale with the lowest and highest features on the image being black and white, respectively. The height scales are specified in the figure captions. Due to instrumental artifacts caused by the curvature of piezoelectric ceramic when it scans over a large area, appropriate flattening was applied to the AFM images. This is the only data treatment applied to our AFM images. The thin film samples were prepared by soaking of precleaned silicon/silicon dioxide wafers in piranha into solutions of copolymers for 24 h, rinsed with hexane and dried with stream of N_2. For scanning electron microscopy (SEM) characterization a small amount of the material was dissolved in THF, the solution was then applied to a specimen disk and the solvent was removed by evaporation. Once the polymer film was dried it was coated with a thin gold film and analyzed using a Jeol JSM 5300 scanning electron microscope using a 5 kV electron beam to obtain SEM images of various magnifications.

2.1.1. Macroligand initiator (*2*)

A mixture of 5.2 g (0.18 mmol) of (**1**) and 1.22 mL (8.80 mmol) of triethylamine in 25 mL of dry dichloromethane was cooled to 0 °C in an ice bath for 30 min. 2.7 mL (22 mmol) of 2-bromoisobutyryl bromide was added dropwise and was allowed to react under vigorous stirring overnight at room temperature. The reaction product was filtered through a Celite pad and copiously washed with dichloromethane and, successively with 3% $NaHCO_3$ (2×30 mL), water (2×30 mL) and dried over Na_2SO_4. After concentrating the product solution, it was precipitated by adding the solution dropwise into vigorously stirring diethyl ether solution. The resulting off white precipitate was then collected and dried under vacuum. Yield 3.9 g (78%).

^1H NMR (DMSO-d_6, δ in ppm) δ: 8.61 (d, broad, H6′ of bpy), 8.55 (d, broad, H6 of bpy), 8.38 (s, broad, H3′ of bpy), 8.28 (s, broad, H3 of bpy), 7.13–7.18 (d, broad, H5′ and H5 of bpy), 5.23 (s, broad, CH_2O of bpy), 4.07 (m, broad, CH_2O of PCL), 2.33 (m, broad, $OCCH_2$ of PCL), 1.97 (s, $C(CH_3)_2$), 1.64 (m, broad, CH_2, of PCL), 1.39 (m, broad, CH_2 of PCL). IR (KBr pellets, ν in cm^{-1}) ν: 3439 (s, broad, OH str), 2951

(m, sharp, arom C–H str), 2857 (m, sharp, aliph C–H str), 2095–2019 (m, broad, arom overtone bands), 1719 (s, sharp, C=O ester str), 1594 (s, sharp, C=C ring str), 1471 (m, sharp, arom C–N str), 1100 (s, broad, C–O–C str), 849 (s, sharp, arom out-of-plane bend). GPC (LALLS). M_w: 27,900, M_w/M_n: 1.28

2.1.2. MebpyPCL-b-styrene (4)

A flame dried schlenk flask with a three way valve was charged in 7.6 mg (0.011 mmol) of (**3**), 6.8 mg (0.032 mmol) of tricyclohexylphosphine (Pcy_3), in 4 mL of *N*-methylpyrrolidione (NMP) and was stirred under N_2 atmosphere until a homogeneous solution was obtained. 0.52 g (0.012 mmol) of initiator (**2**), and 2.3 g (19 mmol) of styrene in 5 mL of *N*-methylpyrrolidione (NMP) were then added to the complex catalyst mixture and left to react in preheated oil bath for 6 h at 85–90 °C. The reaction mixture was cooled, diluted with THF and filtered through neutral alumina. It was precipitated in cold heptane and vacuum dried. Yield 0.75 g (86%) off-white polymer.

^{1}H NMR ($CDCl_3$, δ in ppm) δ: 6.45–7.26 (m, broad, PS ArH), 5.21 (s, broad, CH_2O bpy), 4.08 (broad, CH_2O of PCL), 2.30 (m, broad, $OCCH_2$ of PCL), 1.34–1.74 (complex m, CH_2 PCL and PS chain). IR (KBr pellets, ν in cm^{-1}) ν: 2954 (m, sharp, arom C–H str), 2865 (m, sharp, aliph C–H str), 1890–1730 (m, broad, arom overtone bands), 1729 (s, sharp, C=O ester str), 1592 (s, sharp, C=C ring str), 1445 (m, sharp, arom C–N str), 1088 (s, broad, C–O–C str), 739 (s, sharp, C–H arom out-of-plane bend). GPC (LALLS). M_w: 44,000, M_w/M_n: 1.37

2.1.3. Ru(bpy)$_2$(mebpyPCL)-b-styrene (PF_6)$_2$ (5)

3.6 mg (8.2 μmol) of *cis*-$Ru(bpy)_2Cl_2$ were dissolved in 20 mL of methanol, 3.2 mg (19.3 μmol) of $AgNO_3$ were added to the dissolved substrate and the solution was left stirring for 2 h at room temperature. The resulting white precipitate was filtered off and evaporated to dryness and then redissolved in 10 mL of acetonitrile/dimethoxyethanol (DME) (1:1) mixture. To this was added 0.3 g (8 μmol) of macroligand polymer (**4**) and refluxed for 24 h with vigorous stirring. The solvent was then removed using a rotary evaporator and the resulting red–orange product was purified by column chromatography (silica) using methylene chloride as the eluent. After reducing the solvent volume to 5–10 mL, the product was precipitated by addition with stirring to a methanolic potassium hexafluorophosphate solution. The product was then filtered, washed with ether and vacuum dried. Yield 0.26 g (72%) of red–orange polymer.

^{1}H NMR ($CDCl_3$, δ in ppm) δ: 6.45–7.26 (m, broad, PS ArH), 5.27 (s, broad, CH_2O bpy), 4.08 (broad, CH_2O of PCL), 2.30 (m, broad, $OCCH_2$ of PCL), 1.34–1.78 (complex m, CH_2 PCL and PS chain). IR (KBr pellets, ν in cm^{-1}) ν: 2939 (m, sharp, arom C–H str), 2872 (m, sharp, aliph C–H str), 1890–1730 (m, broad, arom overtone bands), 1725 (s, sharp, C=O ester str), 1598 (s, sharp, C=C ring str), 1447 (m, sharp, arom C–N str), 1097 (s, broad, C–O–C str), 724 (s, sharp, C–H arom out-of-plane bend). UV–vis ($CHCl_3$) λ_{max}: 288 nm (ε = 75,300 M^{-1} cm^{-1}), 454 nm (ε = 11,600 M^{-1} cm^{-1}). GPC (LALLS). M_w: 44,600, M_w/M_n: 1.39

3. Results and discussion

3.1. Synthesis

Macroligand initiator (**2**) was obtained by the reaction of hydroxyl reactive polymer (**1**) with 2-bromoisobutyryl bromide in the presence of triethylamine in dichloromethane. The bromoester macroligand (**2**) was characterized by ^{1}H NMR, ^{13}C NMR and gel permeation chromatography (GPC). The ^{1}H NMR spectrum of (**2**) showed a sharp singlet at 1.97 ppm for the $C(CH_3)_2(Br)$ methyl signals in addition to characteristic signals of bipyridine and poly(ε-caprolactone), with no residual protons of the starting material as shown in Fig. 1 (top spectrum). Polymer (**2**) revealed no change of polymer molecular weight and molecular distribution with respect to parent polymer (**1**). Macroligand initiator (**2**) was then utilized for the ATRP of styrene in the presence of in situ generated catalyst of the type $[RuCl_2(\eta^6\text{-cymene})(L)]$ (L = Pcy_3 tricylcohexylphosphine). Bulk polymerization of styrene with macroinitiator (**2**) afforded poly(ε-caprolactone)-*b*-polystyrene diblocks with short styrene segments and multimodal GPC traces presumable due to chain transfer reactions. The use of solvent such as *N*-methylpyrrolidione (NMP) enhanced the miscibility of the metal complex catalyst and provided polymers with molecular weights that corresponded to the expected ones.

Overlay GPC traces of macroinitiator (**2**) and the metal free copolymer (**4**) are shown in Fig. 2. For the diblock (**4**), the GPC analysis exhibited a decrease in elution time with little change in molecular weight distribution corresponding to the increased molecular weight as expected. Furthermore, the ^{1}H NMR analyses has allowed the identification of characteristic peak resonances attributable to the functional poly(ε-caprolactone) macroinitiator as well as that of styrene components in the diblock (Fig. 1 (bottom spectrum)). By integrating the ^{1}H NMR polystyrene resonance peaks (PS-H) and that of poly(ε-caprolactone) macroligand initiator (OCH_2) and taking into account the number average molecular weight of PCL macroligand initiator determined via GPC (LALLS), a molecular weight of (42,000 g mol^{-1}) was obtained for diblock (**4**). The agreement between the ^{1}H NMR and GPC (LALLS) (44,000 g mol^{-1}) molecular weight determination for the diblock (**4**) is fairly good and would suggest that it contains PCL_{250}-*b*-PS_{145} homopolymeric sequence, respectively. Nevertheless, the absence of the characteristic bipyridine signals in the ^{1}H NMR spectrum in the diblock (**4**) due to increase of its molecular weight is similar to what has been previously reported for other bpy macroligands [24]. These results further support the effectiveness of the polyester end grafting and the successful introduction of the second styrene segment into the poly(ε-caprolactone) macroinitiator chain, using this in situ generated ruthenium based catalysis system. The linear metallated poly(ε-caprolactone)-*b*-polystyrene diblock (**5**) bearing $[Ru(bpy)_3]^{2+}$chromophores was obtained via macroligand-chelation method [25]. Basically, this method is an extension of normal chelation reactions of small molecules and metal ion precursor in standard inorganic

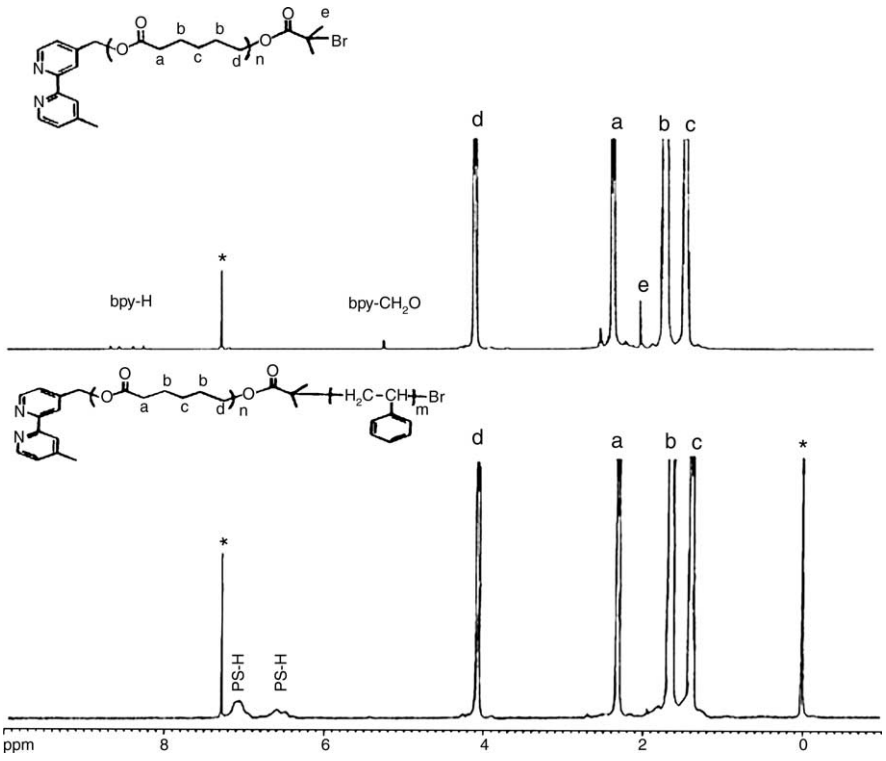

Fig. 1. ^{1}H NMR spectra of macroligand initiator (**2**) and copolymer (**4**). (*) denotes the $CDCl_3$ solvent and the TMS reference.

reactions [26]. However, it is generally difficult to extrapolate chemistry from inorganic/organic synthesis to polymer reactions, because the kinetics are usually different for each case. Polymer chain entanglement always limits the collision between active coordination sites in the polymer and the metal ions. In the case of high molecular weight polymeric macroligands, additional reaction parameters have to be taken into account [27]. The reaction medium must be capable of efficiently solubilizing both the metal ion precursors and the polymeric macroligand undergoing the substitution. More importantly, the solvent has to facilitate ligand substitution by solvating leaving groups or by providing labile metal ion solvent coordinated intermediates, making the metal centers sites prone to facile coordination. Macroligand solution phenomena, such as chain conformation and aggregation have to be considered as well [28]. Thus, in the macroligand-chelation method for the preparation of poly(ε-caprolactone)-*b*-polystyrene diblock (**5**) with $[Ru(bpy)_3]^{2+}$ luminescent centers at one polymer termini, *cis*-$Ru(bpy)_2Cl_2$ precursor was first dehalogenated with $AgNO_3$ in methanol. After AgCl removal, the resulting $[Ru(bpy)_2(MeOH)_2]^{2+}$ solvent coordinated metal precursor was reacted with polymeric macroligand (**4**) in a acetonitrile/DME (1:1 v/v) solvent to generate the desired polymer after chromatography and repeated purification cycles.

3.2. Thermal analysis

Thermal transition parameters and thermal stabilities of the poly(ε-caprolactone) macroligand (**1**), macroligand initiator (**2**), the metal free (**4**) as well as the metal anchored diblock (**5**) were determined by using differential scanning calorimetry (DSC) and thermogravimetric analysis (TGA) under N_2 atmosphere. As a representative example the DSC thermogram of the metal free diblock (**4**) is shown in Fig. 3. A weak glass transition temperature of the amorphous domains of the poly(ε-caprolactone) at −63 °C (inset) and sharp melting endotherm at around 58 °C, corresponding to the melting temperature of the semicrystalline poly(ε-caprolactone) segments were only observed. The expected glass transition temperature of the amorphous styrene domains at 105 °C in the diblock (**4**) was not evident in the DSC thermogram, presumably due to the miscibility of the two homopolymers in the melt. Thermal transition parameters remain unaffected as indicated by the

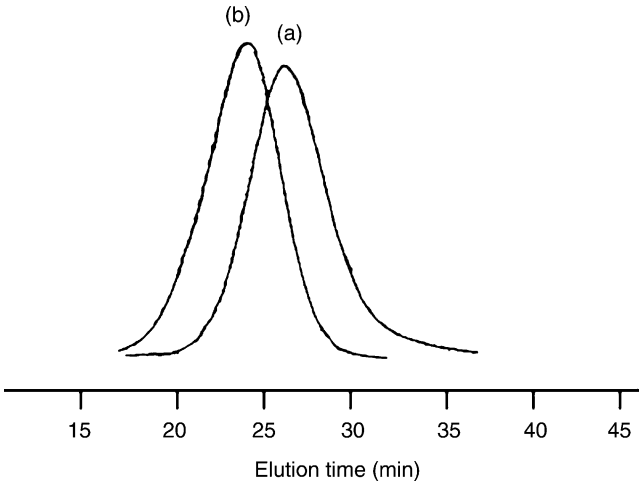

Fig. 2. Overlay GPC traces of (a) macroligand initiator (**2**) and (b) copolymer (**4**).

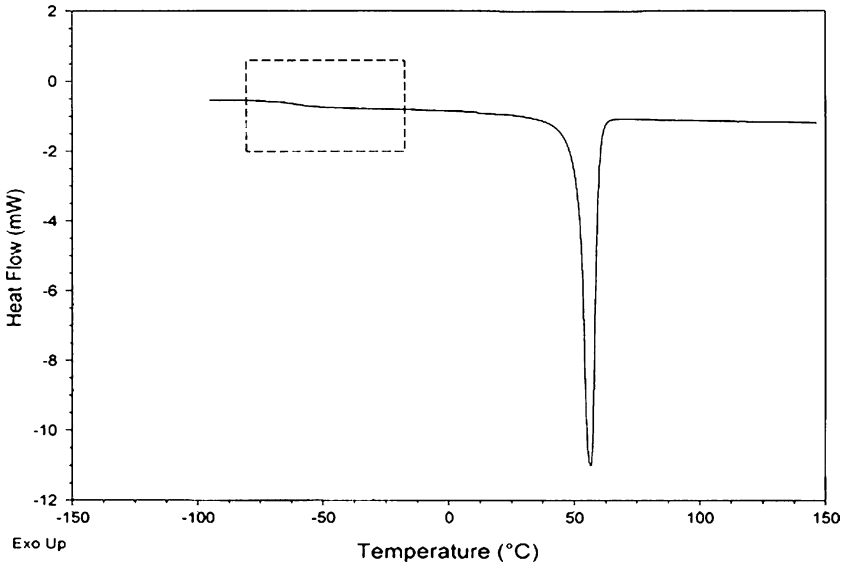

Fig. 3. DSC thermogram of copolymer (**4**). Inset refers to the glass transition temperature of poly(ε-caprolactone).

DSC thermograms for the diblocks (**4**) and (**5**) irrespective of metal presence in the diblock microstructures. However, the thermogravimetric analyses (TGA) showed similar and high thermal stabilities for the metal free diblock (**4**) and the metallo-diblock (**5**) with respect to homopolymers (**1**) and (**2**) as supported by an increase of about 50 °C in temperature for the onset of their thermal degradation trend. As representative example an overlay TGA thermogram for the diblock (**4**) and homopolymer macroinitiator (**2**) is shown in Fig. 4. In analogy to the DSC analyses, TGA analyses have also revealed no effect of the metal presence to the overall thermal stabilities for the diblocks (**4**) and (**5**). Hence, the observed increase in temperature for the initial degradation pattern for the diblocks (**4**) and (**5**) with respect to the homopolymers (**1**) and (**2**) could, therefore, be solely attributed to the increase of their molecular weight.

3.3. Absorption and emission spectroscopy of the metal-centered copolymer

An intense ligand centered band at 290 nm followed by a metal-to-ligand charge transfer (MLCT) absorption at 460 nm typical of the polypyridyl Ru chromophores [29] was evident in the UV–vis spectra of the Ru anchored diblock (**5**). The copolymer also revealed an emission band at around 610 nm characteristic of (MLCT) emission of $[Ru(bpy)_3]^{2+}$

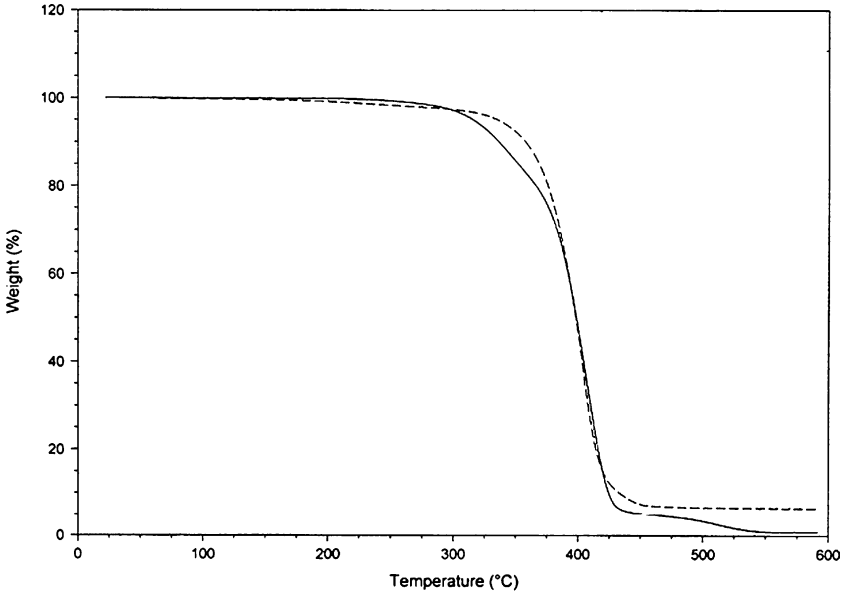

Fig. 4. Overlay TGA thermograms of macroligand initiator (**2**) (dotted lines) and copolymer (**4**) (solid lines) under N_2 atmosphere.

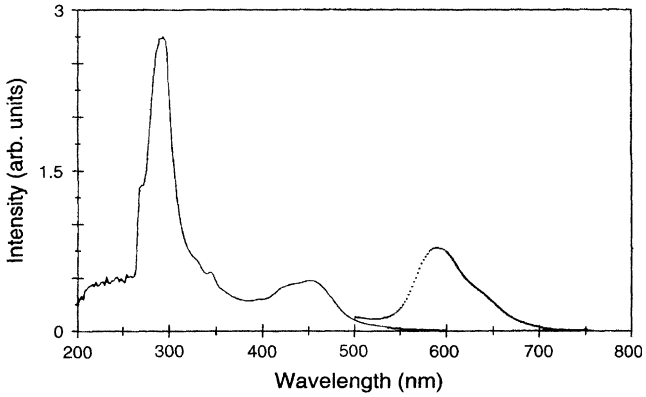

Fig. 5. UV–vis and emission spectra of diblock (**5**) in deoxygenated chloroform.

chromophores after an excitation at 400 nm in deareated chloroform solution as shown in Fig. 5. These observed electronic and emission spectral features are in consistent with the presence of $[Ru(bpy)_3]^{2+}$ metal chromophores in the metallo-diblock (**5**) as expected.

3.4. Polymer modified surfaces

The surface morphology of thin film of macroligand initiator (**2**) and the metal free diblock (**4**) onto silicon wafers were obtained using atomic force microscopy (AFM) in tapping mode and scanning electron microscopy (SEM). All AFM images were taken from dry surfaces at room temperature under air atmosphere. To rule out the presence of image artifacts, trace and retrace AFM scans were compared for the surface-modified samples. The images were found to be identical; after multiple scans, demonstrating that the tip did not alter the surface topology. In Fig. 6(a) and (b), the height mode AFM image of the macroligand initiator (**2**) is shown for two areas of the film displaying different coverage. Initially the polymer chains exist as bright semicrystalline random coils and amorphous elongated features that are of similar morphology to what is expected for linear polymers [30]. Poly(ε-caprolactone) is known to be semicrystalline materials with coexisting regions of amorphous and crystalline domains. The observed bright aggregates in Fig. 6(a) and (b) are assigned to poly(ε-caprolactone) domains that are concentrating at the top surface due to their hydrophobicity and lower surface energy (due to the hydrophilic Si oxide surface). In many cases for semicrystalline polymer, it is the combination of total crystallinity and crystallite morphology that dictate their end use properties. The thermal treatment of semicrystalline polymers is known to have a strong effect on both the morphology of crystalline domains and the details of the amorphous regions. Hence, morphology inducible effects such as annealing the semicrystalline homopolymer (**2**) and the diblock (**4**) to trigger a crystallite formation with concurrent microphase separation at the nanometer scale were investigated.

AFM image of annealed macroligand initiator (**2**) at 40 °C under N_2 atmosphere is reported in Fig. 6(c) and (d). The amorphous poly(ε-caprolactone) domains that are above their glass transition temperature are now allowed to crystallize and, therefore, the polymer chains tend to relax and change their conformation, forming globular or interconnected highly crystalline spherulites. In contrast to macroligand initiator

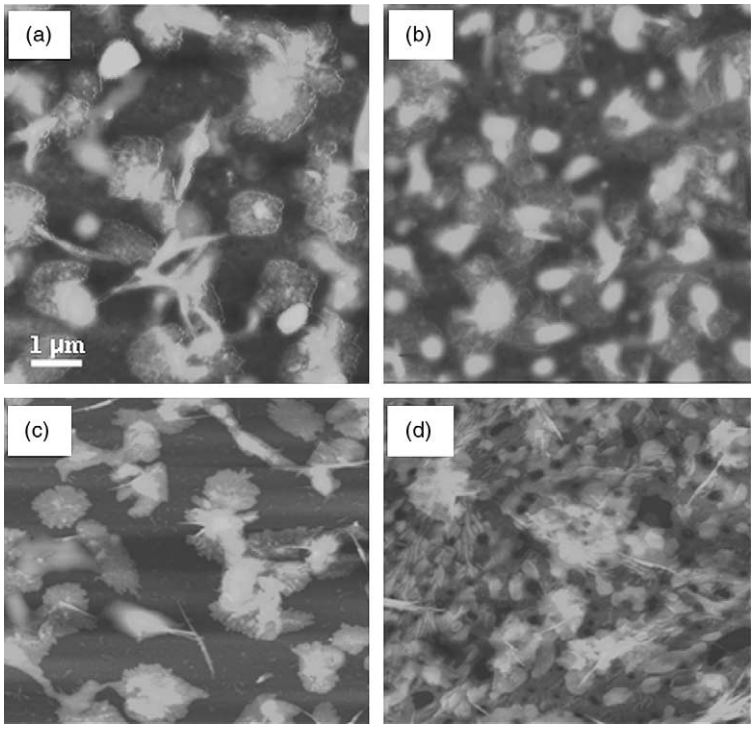

Fig. 6. Tapping mode AFM images of macroligand initiator (**2**) on Si/SiO_2 surface. (a) and (b) as prepared and (c) and (d) after annealing at 40 °C under N_2 atmosphere. The height scale and scan size are the same for all the images and were set to 140 nm and 5×5 μm^2.

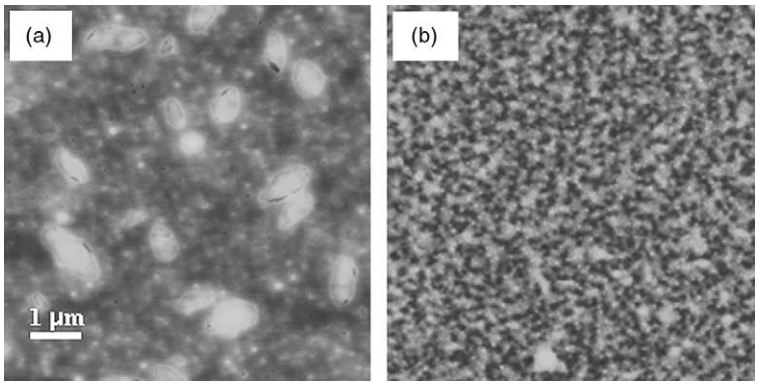

Fig. 7. (a) Tapping mode AFM images of copolymer (**4**) on Si/SiO_2surface (a) as prepared and (b) after annealing at 40 °C under N_2 atmosphere. The height scale and scan size are the same for all the images and were set to 50 nm and 5×5 μm^2.

(**2**), poly(ε-caprolactone)-*b*-polystyrene diblock films (**4**) display as shown in Fig. 7(a), separate-globular features possibly consisting of entangled amorphous/semicrystalline segments. When annealed samples are visualized under AFM as in Fig. 7(b), a disrupted crystalline morphology with intermixed amorphous/semicrystalline dendrimer—like domains was observed. These observed morphologies are expected for AB type diblock copolymers since the structures follow the predictions for the linear block copolymer [31]. The difference in surface morphology of thin films between PCL macroinitiator (**2**) and that of metal free poly(ε-caprolactone)-*b*-polystyrene (**4**) diblock films was also studied using scanning electron microscopy (SEM). Rough lamellar stacks characteristic of semicrystalline domains of PCL macroinitiator (**2**) and very smooth surface morphology with no apparent crystalline morphology for poly(ε-caprolactone)-*b*-polystyrene diblock

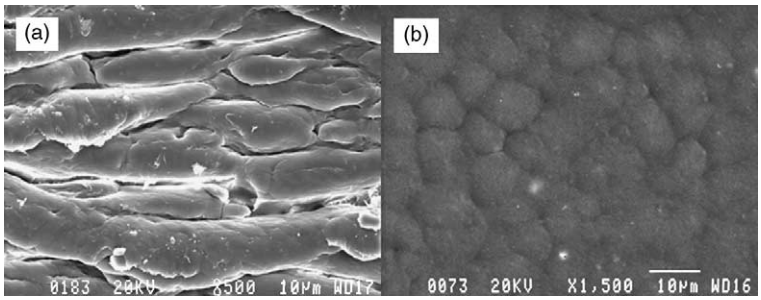

Fig. 8. SEM images of (a) macroligand initiator (**2**) (magnification: 500 times) and (b) copolymer (**4**) (magnification 1500 times).

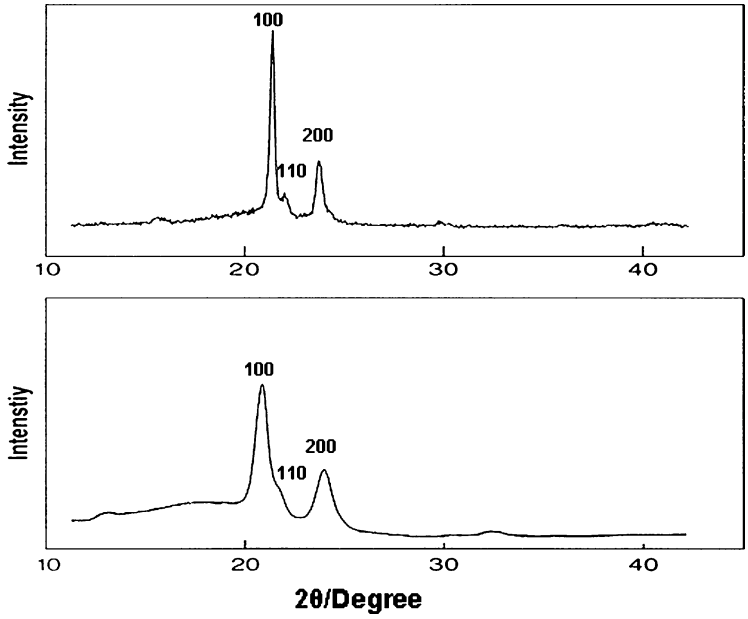

Fig. 9. (a) WAXD pattern of macroligand initiator (**2**) (top) and (b) copolymer (**4**) (bottom).

(**4**) were revealed in the SEM images as shown in Fig. 8(a) and (b), respectively. The observed disruption of recrystallization and the degree of molecular order of the PCL macroinitiator upon grafting of styrene blocks was further supported by wide angle X-ray diffraction (WAXD) studies. As shown in Fig. 9, the PCL macroinitiator (**2**) shows sharp and high intensity peaks in the 2θ region between 20 and 30°. In the same region, the poly(ε-caprolactone)-*b*-polystyrene diblock (**4**) showed broad and intensity reduced reflection peaks, suggesting a lower degree of crystallization in the diblock. In either case, the observed WAXD reflections for both samples demonstrate crystallographic patterns that were indexed to the known semicrystalline poly(ε-caprolactone) diffraction data [32].

4. Conclusion

A versatile telechelic macromonomer initiator (**2**) was synthesized, characterized and then subjected to solution atom transfer radical polymerization (ATRP) of styrene with in situ generated catalyst via $[RuCl_2(\eta^6\text{-cymene})]_2$ dimer complex. The resulting linear poly(ε-caprolactone)-*b*-polystyrene metal free diblock (**4**) and the corresponding metallated (**5**) species were readily isolated without any time-consuming separation and purification steps. These polymers were then characterized by multitude of analytical techniques, i.e. gel permeation chromatography (GPC) coupled with low-angle laser light scattering (LALLS), ^{1}H NMR, FT-IR, UV/vis spectroscopy, differential scanning calorimetry (DSC) and thermogravimetric analysis (TGA). All these techniques have confirmed the properties and the desired molecular structures of the diblocks. Furthermore, imaging techniques such as atomic force microscopy (AFM) and scanning electron microscopy (SEM) of thin films of the metal free diblock in conjunction with WAXD analyses have indicated the reduced crystallization tendency of the semicrystalline poly(ε-caprolactone) macroligand initiator due to chain end grafting of amorphous styrene segments. Moreover, the synthesis of multifunctional macromolecules bearing Ru (II) chromophores in well-defined polymer chain termini was also achieved. The coordination chemistry of the vacant bpy coordination sites of the metal free diblock macroligand (**4**) with other metals or metal ion precursors has its own merit for further studies. It could potentially provide a wide of range of functionalized metallomacromolecules of tailored properties and widens the horizon of research interest and the application of transition metal containing polymers as well.

Acknowledgements

This work was financially supported by the Natural Sciences and Engineering Research Council (NSERC) of Canada and York University. We thank to Prof. Ian Manners and his research group (Chemistry Department at University of Toronto) for their assistance in GPC and TGA analyses. S. M acknowledges support from Canada Research Chair program and from Canadian Foundation for Innovation and Ontario Innovation Trust.

References

[1] (a) Noshay A, McGarth JE. Block copolymers: overview and critical survey. New York: Academic Press; 1977.
(b) Reiss G, Hurtrez C, Bahadur P. Block copolymers. In: Mark HF, Bikales NM, Overberger CG, Menges G, editors. Encyclopedia of polymer science and engineering. 2nd ed. New York: Wiley; 1985.
(c) Hazer B. Synthesis and characterization of block copolymers. Cheremsinoff NP (Eds) Handbook of polymer science and technology. New York: Marcel Dekker, p. 133 [chapter IV].
(d) Fasolka MJ, Mayes AM. Annu Rev Mater Res 2001;31:323.
(e) Park C, Yoon J, Thomas EL. Polymer 2003;44:6725.
[2] Richards DH. Chem Soc Rev 1977;6:235.
[3] Michiharu Y, Fumiko N, Tomoko D, Yutaka M. J Int Adhes Adhes 2002; 22:37.
[4] Katsuura H, Kawamura H, Manabe M, Kawasaki H, Maeda H. Colloid Polym Sci 2002;280:710.
[5] Thombre S. J Appl Polym Sci 2002;86:1211.
[6] Balaji R, Nanjunolan S. J Appl Polym Sci 2002;86:1023.
[7] Wright T, Jones AS, Harwood HJ. J Appl Polym Sci 2002;86:1203.
[8] Jonquires A, Clement R, Lochon P. Prog Polym Sci 2002;27:1803.
[9] Atta AM, Arndt KF. J Appl Polym Sci 2002;86:1138.
[10] Goboyard M, Hervaud Y, Boutevin B. Polym Int 2002;51:577.
[11] Coates G, Hustad PD, Reinarts S. Angew Chem, Int Ed 2002;41:2236.
[12] (a) [Reviews on ATRP see] Patten TE, Matyjaszewski K. Adv Mater 1998;10:901.
(b) Coessens V, Pintauer T, Matyjaszewski K. Prog Polym Sci 2001;26:337.
(c) Sawamoto M, Kamigaito M. Trends Polym Sci 1996;4:371.
(d) Sawamoto M, Kamigaito M. Synthesis of polymers. In: Schulter AD, editor. Materials science and technology series. Weinheim: Wiley; 1998 [chapter 6].
(e) Sawamoto M, Kamigaito M. Chemtech 1999;29:30.
(f) Matyjaszewski K, Xia J. Chem Rev; 2001:2921.
(g) Patten TE, Matyjaszewski K. Acc Chem Res 1999;32:895.
(h) Grozinski J. J React Funct Polym 2001;49:1.
[13] (a) [For a general review of metal-containing polymers see:] Carraher Jr CE, Sheats JE, Pittman Jr CU, editors. Organometallic polymers. NY: Academic Press; 1978.
(b) Sheats JE, Carraher Jr CE, Pittman Jr CU, editors. Metal containing polymeric systems. NY: Plenum; 1985.
(c) Sheats JE, Carraher Jr CE, Pittman Jr CP, Zeldin M, Currel B, editors. Inorganic and metal-containing polymeric materials. NY: Plenum; 1985.
(d) Zeldin M, Wynne KJ, Allcock HR, editors. Inorganic and organometallic polymers. ACS Symposium Series; 1988. p. 360.
(e) Cullbertson BM, Pittman Jr CU. New monomers and polymers. NY: Plenum; 1984.
(f) Neuse EW, Rosenberg H. Metallocene polymers. NY: Marcel-Dekker; 1970.
(g) Sheats JE. Kirk-Othmer encyclopedia of chemical technology, 3rd ed, vol. 15. NY: Wiley; 1981.
(h) Manners I. Adv Organomet Chem 1995;37:131.
[14] (a) Manners I. J Polym Sci, Part A: Polym Chem 2002;40:179.
(b) Kulbaba K, Manners I. Macromol Rapid Commun 2001;22:711.
[15] (a) Abd-El-Aziz AS. Coord Chem Rev 2002;233–234:177.
(b) Pickup PG. J Mater Chem 1999;9:1641.
[16] (a) Schubert US, Eschbaumer C. Angew Chem, Int Ed 2002;41:2892.
(b) Schubert U, Heller M. Chem Eur J 2001;7:5253.
[17] (a) Simal F, Demonceau A, Noels AF. Angew Chem Int Ed 1999;38:538.
(b) Delaude L, Demonceau A, Noels AF. Chem, Commun 2001;986.
[18] Fraser CL, Smith AP. J Polym Sci, Part A: Polym Chem 2000;38:4704 [and references there in].
[19] Farah AA, Pietro W. J Can J Chem 2004;82:595.
[20] Ando T, Kamigato M, Sawamoto M. Tetrahedron 1997;53:15445.

[21] Perrin DD, Armarego WLF, Perrin DR. Purification of laboratory chemicals. 2nd ed. New York: Pergamon Press; 1980.
[22] (a) Sullivan BP, Salmon DJ, Meyer T. J Inorg Chem 1978;17:3334.
(b) Veinot JGC, Farah AA, Galloro J, Zobi F, Bell V, Pietro W. J Polyhedron 2000;19:331.
[23] (a) Zelonka RA, Baird MC. Can J Chem 1972;50:3063.
(b) Inorganic synthesis. vol. XXI, Wiley: New York; 1982, p. 75.
[24] (a) McAlvin JE, Scott SB, Fraser CL. Macromolecules 2000;33:6953.
(b) Wu X, Fraser CL. Macromolecules 2000;33:4053.
[25] (a) Corbin PS, Webb MP, McAlvin JE, Fraser CL. Biomacromolecules 2001;2:223.
(b) Smith AP, Fraser CL. Macromolecules 2002;35:594.
(c) Smith AP, Fraser CL. Macromolecules 2003;36:2654.
[26] Cotton FA, Wilson G, Murillo CA, Bochmann M. Advanced inorganic chemistry. 6th ed. New York: Wiley & Sons; 1999.
[27] (a) Wu X, Fraser CL. Macromolecules 2000;33:7776.
(b) Fraser CL, Smith AP, Wu X. J Am Chem Soc 2000;122:9026.
[28] Heise A, Hedrick JL, Frank CW, Miller RD. J Am Chem Soc 1999;121:8647.
[29] Ford P, De Rudd FP, Guander R, Taube H. J Am Chem Soc 1968;90:1187.
[30] Bassett DC. Principles of polymer morphology. New York: Cambridge University Press; 1981.
[31] Milner ST. Macromolecules 1994;27:2333.
[32] (a) Rhee S-H, Choi J-Y, Kim H-M. Biomaterials 2002;23:4915.
(b) Huang M-H, Li S, Vert M. Polymers 2004;26:8675.